

# Photon-assisted electron transport in graphene

B. Trauzettel,<sup>1,2</sup> Ya. M. Blanter,<sup>3</sup> and A. F. Morpurgo<sup>3</sup>

<sup>1</sup>*Instituut-Lorentz, Universiteit Leiden, P.O. Box 9506, 2300 RA Leiden, The Netherlands*

<sup>2</sup>*Department of Physics and Astronomy, University of Basel, Klingelbergstrasse 82, 4056 Basel, Switzerland*

<sup>3</sup>*Kavli Institute of Nanoscience, Delft University of Technology, Lorentzweg 1, 2628 CJ Delft, The Netherlands*  
(Dated: September 2006)

Photon-assisted electron transport in ballistic graphene is analyzed using scattering theory. We show that the presence of an ac signal (applied to a gate electrode in a region of the system) has interesting consequences on electron transport in graphene, where the low energy dynamics is described by the Dirac equation. In particular, such a setup describes a feasible way to probe energy dependent transmission in graphene. This is of substantial interest because the energy dependence of transmission in mesoscopic graphene is the basis of many peculiar transport phenomena proposed in the recent literature. Furthermore, we discuss the relevance of our analysis of ac transport in graphene to the observability of *zitterbewegung* of electrons that behave as relativistic particles (but with a lower effective speed of light).

PACS numbers: 73.23.Ad, 73.23.-b, 73.63.-b, 03.65.Pm

## I. INTRODUCTION

Since the discovery of an anomalous quantum Hall effect in graphene [1, 2], promising possibilities to observe quantum dynamics of Dirac fermions in such systems have been proposed. The most prominent one is the quantum-limited conductivity (of order  $e^2/h$ ), where measurements [1, 2] and theoretical predictions [3, 4, 5, 6, 7, 8] are still inconsistent with each other. Other examples of unusual quantum transport phenomena in mesoscopic graphene are a maximum Fano factor of  $\frac{1}{3}$  [9], selective transmission of Dirac electrons through  $n$ - $p$  junctions [10], the phenomenon of Klein tunnelling [11], and transport phenomena at interfaces between graphene and a superconductor [12, 13, 14, 15]. Recently, the effect on the longitudinal and Hall conductivity of an applied microwave signal has been analyzed in bulk graphene [16]. In many of these works, interesting phenomena arise because transport through graphene is in general energy dependent. Therefore, it is desirable to directly probe the energy dependence of transport. We show that the Tien-Gordon problem [17, 18] of photon-assisted electron transport for Dirac electrons is a powerful tool to quantitatively probe energy dependent transmission in graphene. The idea is to apply an ac signal to a region of graphene and a bias with respect to a neighboring region to allow electron transport from the one to the other (see Fig. 1) [19].

In the dc limit, electron transport then allows to directly determine the energy dependent transmission coefficients of the underlying scattering problem. Additionally, we find that resonance phenomena (sharp steps in  $dG/dV$ , where  $G = dI/dV$  is the differential conductance) arise if the applied bias  $V$  equals multiples of the applied ac frequency  $\omega$ . These resonance phenomena are due to the vanishing of propagating modes directly at the Dirac point (the point in the spectrum of graphene, where the valence band and the conduction band touch each other). This implies an interesting application of

graphene: It can be used as a spectrometer for high frequency noise – similar to the superconductor–insulator–superconductor (SIS) junction in Ref. [20] with the advantage that there is no frequency limit.

Another motivation to look at the Tien-Gordon problem in graphene is its relevance to the observability of an interesting and unobserved phenomenon, present for free Dirac fermions but absent for free Schrödinger fermions, called *zitterbewegung* (ZB) [21, 22]. ZB manifests itself, for instance, in a time-dependent oscillation of the position operator of a Dirac electron in the Heisenberg picture. A pioneering attempt to describe an experimental way to observe ZB in III–V semiconductor quantum wells has been proposed in Ref. [23]. Others have adopted this idea to carbon nanotubes [24], spintronic, graphene, and superconducting systems [25]. Another situation where non-relativistic electrons experience ZB is the presence of an external periodic potential [26]. In fact, there is a wide class of Hamiltonians (where the corresponding wave function is a spinor) which all exhibit ZB [27]. Nevertheless – although almost omnipresent – the phenomenon has never been observed in nature. Therefore, it is desirable to propose an unambiguous signature of ZB in a particular setup. As we show below, the conditions to observe ZB can be easily created using the Tien-Gordon effect, which results in an oscillating current due to the existence of a wavefunction that is a superposition of different energies. However, an unambiguous detection of ZB in this way is complicated, since also for the free Schrödinger equation an oscillating current is generated when the wavefunction is a superposition of different energies. Additional studies are needed to single out effects of ZB and ensure their unambiguous observation.

The paper is organized as follows: In Sec. II, we introduce the setup under consideration and the model to describe it. The photon-assisted current is analyzed in Sec. III. Afterwards, in Sec. IV, we discuss the relevance of the previous analysis to the observability of ZB in graphene. Finally, we conclude in Sec. V.

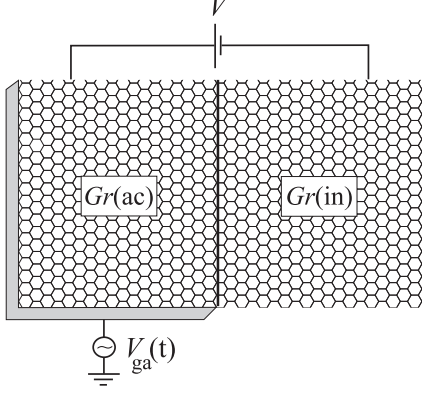


FIG. 1: Schematic of the setup. Two regions of graphene (called  $Gr(ac)$  and  $Gr(in)$ ) are voltage-biased with respect to each other with a bias  $V$ . A gate electrode (grey-shaded area) shifts the Dirac point of region  $Gr(ac)$  away from zero energy. Additionally, a small ac signal is applied to the gate to generate side band transitions. The applied gate voltage  $V_{ga}(t)$  has to be chosen in such a way that the (time-dependent) chemical potential in region  $Gr(ac)$  is given by Eq. (2).

## II. SETUP AND MODEL

The setup under consideration is illustrated in Fig. 1. It contains two regions of graphene called  $Gr(ac)$  and  $Gr(in)$ . A gate electrode in region  $Gr(ac)$  shifts the Dirac points of the two regions with respect to each other by an amount  $eV_S$ . Additionally, we apply a small ac signal to the gate electrode.

An ideal sheet of graphene (in the absence of  $K$ - $K'$  inter-valley mixing) can be described in the effective mass approximation by a two-dimensional Dirac equation (DE) for a two-component wave-function envelope  $\Psi = (\Psi_1, \Psi_2)$  (subscript 1, 2 refers to pseudospins, whose origin can be traced to the presence of two carbon sublattices)

$$\left[ -i\hbar v \begin{pmatrix} 0 & \partial_x - i\partial_y \\ \partial_x + i\partial_y & 0 \end{pmatrix} - \mu(x) \right] \Psi_{e/h} = i\hbar \partial_t \Psi_{e/h}, \quad (1)$$

where  $v$  is the Fermi velocity. The dimensions of the sample are assumed to be large enough such that boundary effects can be neglected. It is, however, straightforward to include boundary effects along the lines of Ref. [9]. The index  $e/h$  refers to electron-like (energy  $\varepsilon > 0$  with respect to the Dirac point) and hole-like (energy  $\varepsilon < 0$  with respect to the Dirac point) solutions to the DE. The chemical potential of the two regions  $Gr(ac)$  ( $x < 0$ ) and  $Gr(in)$  ( $x > 0$ ) is

$$\mu(x) = \begin{cases} eV_S + eV_{ac} \cos(\omega t), & \text{for } x < 0 \\ 0, & \text{for } x > 0 \end{cases}. \quad (2)$$

The potential  $\mu(x)$  is chosen such that a solution to the DE with components of different energies is generated in

$Gr(ac)$  and transmitted to  $Gr(in)$ . The solution to the wave equation (1) for  $x < 0$  (in region  $Gr(ac)$ ) may then be written as

$$\begin{aligned} \Psi_{e/h}^{(ac)}(\vec{x}, t) &= \Psi_{0,e/h}^{(ac)}(\vec{x}, t) e^{-i(eV_{ac}/\hbar\omega) \sin(\omega t)} \\ &= \sum_{m=-\infty}^{\infty} J_m \left( \frac{eV_{ac}}{\hbar\omega} \right) \Psi_{0,e/h}^{(ac)}(\vec{x}, t) e^{-im\omega t}, \end{aligned} \quad (3)$$

where  $\Psi_{0,e/h}^{(ac)}(\vec{x}, t) = \Psi_{0,e/h}^{(ac)}(\vec{x}) e^{\mp i\varepsilon t/\hbar}$  and

$$\left[ -i\hbar v \begin{pmatrix} 0 & \partial_x - i\partial_y \\ \partial_x + i\partial_y & 0 \end{pmatrix} - eV_S \right] \Psi_{0,e/h}^{(ac)} = \pm \varepsilon \Psi_{0,e/h}^{(ac)}. \quad (4)$$

(We have dropped the argument  $\vec{x}$  of the wave function in the latter equation.) In Eq. (3),  $J_m$  is the  $m$ th order Bessel function. From now on, we focus without loss of generality on electron-like solutions only and drop the index  $e$ . This is justified because, in ballistic transport from one region of graphene to another region, particles with a fixed energy  $\varepsilon$  (which can be either positive or negative with respect to the Dirac point) are transmitted and their energy is conserved in the absence of inelastic scattering.

The electron-like plane wave solutions of Eq. (4) can be written as linear combinations of the basis states [12]

$$\Psi_{0,+}^{(ac)} = \frac{e^{iqy + ik_{ac}x}}{\sqrt{\cos \alpha_{ac}}} \begin{pmatrix} e^{-i\alpha_{ac}/2} \\ e^{i\alpha_{ac}/2} \end{pmatrix}, \quad (5)$$

$$\Psi_{0,-}^{(ac)} = \frac{e^{iqy - ik_{ac}x}}{\sqrt{\cos \alpha_{ac}}} \begin{pmatrix} e^{i\alpha_{ac}/2} \\ -e^{-i\alpha_{ac}/2} \end{pmatrix}, \quad (6)$$

where

$$\alpha_{ac} = \arcsin \left( \frac{\hbar v q}{\varepsilon + eV_S} \right), \quad (7)$$

$q$  is the transversal momentum, and  $k_{ac} = (\varepsilon + eV_S) \cos \alpha_{ac} / (\hbar v)$  the longitudinal momentum in region  $Gr(ac)$ . Likewise, electron-like plane wave solutions of Eq. (1) in region  $Gr(in)$  can be written as linear combinations of the basis states

$$\Psi_{0,+}^{(in)} = \frac{e^{iqy + ik_{in}x}}{\sqrt{\cos \alpha_{in}}} \begin{pmatrix} e^{-i\alpha_{in}/2} \\ e^{i\alpha_{in}/2} \end{pmatrix}, \quad (8)$$

$$\Psi_{0,-}^{(in)} = \frac{e^{iqy - ik_{in}x}}{\sqrt{\cos \alpha_{in}}} \begin{pmatrix} e^{i\alpha_{in}/2} \\ -e^{-i\alpha_{in}/2} \end{pmatrix}, \quad (9)$$

with  $\alpha_{in} = \arcsin(\hbar v q / \varepsilon)$  and  $k_{in} = (\varepsilon / \hbar v) \cos \alpha_{in}$ . Now, we solve the transmission problem from region  $Gr(ac)$  to region  $Gr(in)$ . An incoming wave function from region  $Gr(ac)$  is given by

$$\Psi_i^{(ac)}(\vec{x}, t) = \sum_{m=-\infty}^{\infty} J_m \left( \frac{eV_{ac}}{\hbar\omega} \right) \Psi_{0,+}^{(ac)} e^{-i(\varepsilon + \hbar m \omega)t/\hbar}.$$

The reflected wave function in region  $Gr(ac)$  reads

$$\Psi_r^{(ac)}(\vec{x}, t) = \sum_{m=-\infty}^{\infty} r_m J_m \left( \frac{eV_{ac}}{\hbar\omega} \right) \Psi_{0,-}^{(ac)} e^{-i(\varepsilon + \hbar m \omega)t/\hbar},$$

where  $r_m$  is the energy-dependent reflection coefficient. Furthermore, a transmitted wave function in region  $Gr(in)$  can be written as

$$\Psi_{tr}^{(in)}(\vec{x}, t) = \sum_{m=-\infty}^{\infty} t_m J_m \left( \frac{eV_{ac}}{\hbar\omega} \right) \Psi_{+,m}^{(in)} e^{-i(\varepsilon + \hbar m\omega)t/\hbar}, \quad (10)$$

where

$$\Psi_{+,m}^{(in)}(\vec{x}) = \frac{e^{iqy + ik_{in,m}x}}{\sqrt{\cos \alpha_{in,m}}} \begin{pmatrix} e^{-i\alpha_{in,m}/2} \\ e^{i\alpha_{in,m}/2} \end{pmatrix} \quad (11)$$

with

$$\alpha_{in,m} = \arcsin \left( \frac{\hbar v q}{\varepsilon + \hbar m\omega} \right) \quad (12)$$

and  $k_{in,m} = (\varepsilon + \hbar m\omega) \cos \alpha_{in,m} / (\hbar v)$ . In Eq. (10),  $t_m$  is the energy-dependent transmission coefficient. In order to determine  $t_m$  and  $r_m$ , we need to match wave functions at  $x = 0$ , namely

$$\Psi_i^{(ac)}(x=0, y, t) + \Psi_r^{(ac)}(x=0, y, t) = \Psi_{tr}^{(in)}(x=0, y, t).$$

The solutions to the resulting set of equations are

$$r_m = \frac{e^{i\alpha_{ac}} - e^{i\alpha_{in,m}}}{1 + e^{i(\alpha_{ac} + \alpha_{in,m})}}, \quad (13)$$

$$t_m = e^{-i(\alpha_{ac} - \alpha_{in,m})/2} \sqrt{\frac{\cos \alpha_{in,m}}{\cos \alpha_{ac}}} \frac{1 + e^{2i\alpha_{ac}}}{1 + e^{i(\alpha_{ac} + \alpha_{in,m})}},$$

where  $\alpha_{ac}$  is given by Eq. (7) and  $\alpha_{in,m}$  by Eq. (12). It is easy to verify that unitarity holds  $|r_m|^2 + |t_m|^2 = 1$ . Furthermore, Eq. (13) shows that if the angle of incidence is zero ( $q = 0$ ) then all transmission coefficients are 1 and all reflection coefficients vanish. This is known as Klein tunnelling in relativistic quantum dynamics [11].

### III. PHOTON-ASSISTED CURRENT

In order to determine the transmitted current, we need to calculate the current density operator in  $x$ -direction

$$J_x(\vec{x}, t) = ev \Psi^*(\vec{x}, t) \sigma_x \Psi(\vec{x}, t), \quad (14)$$

integrate over a cross section in  $y$ -direction, and over angles of incidence. In the following, we assume that a dc bias  $V$  is applied between regions  $Gr(ac)$  and  $Gr(in)$  and that  $k_B T$  is the lowest of all energy scales. The average current is then given by

$$I = \frac{4e}{h} \frac{W}{\pi} \int_0^{q_{\max}} dq \int_0^{eV} d\varepsilon \sum_{m,m'=-\infty}^{\infty} J_m \left( \frac{eV_{ac}}{\hbar\omega} \right) J_{m'} \left( \frac{eV_{ac}}{\hbar\omega} \right) t_m^* t_{m'} e^{i(m-m')\omega t}, \quad (15)$$

where  $W$  is the width of the sample and  $q_{\max} = \min\{|eV + \hbar m\omega|/\hbar v, |eV + eV_S|/\hbar v\}$  is the upper bound

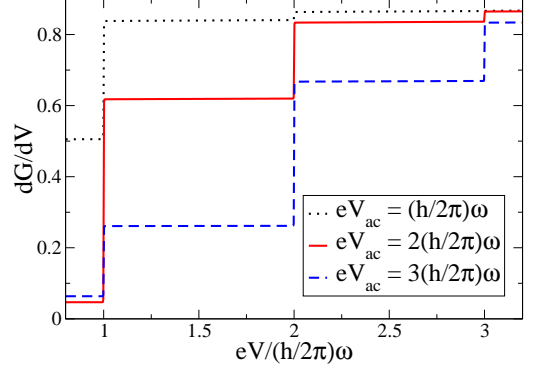


FIG. 2: (Color online)  $dG/dV$  is plotted in units of  $8e^3 W/(v\hbar^2)$  for a fixed value of  $eV_S/\hbar\omega = 100$  and different values of  $eV_{ac}/\hbar\omega$ . Sharp steps appear when the applied bias equals multiples of the ac frequency. The size of the steps is non-universal. It depends on the weight of the different side bands given by the Bessel functions in Eq. (16). For the given values of  $eV_{ac}/\hbar\omega$ , it is sufficient to include side bands up to  $|m| = 4$  to calculate  $dG/dV$  to a very high accuracy.

of the transversal momentum of propagating modes. The bias is applied such that the Fermi function (at zero temperature) in region  $Gr(ac)$  reads  $f_{ac}(E) = \theta(eV - E)$  and, in region  $Gr(in)$ ,  $f_{in}(E) = \theta(-E)$ , where  $\theta(x)$  is the Heaviside step function. Since the scattering matrix is energy-dependent, the current  $I$  depends on the way the bias is applied and not just on its magnitude  $V$ . A factor 4 has been added to the right hand side of Eq. (15) to take into account for spin and valley degeneracy. Apparently, there are terms in Eq. (15) that do not depend on time (where  $m = m'$ ) and terms that oscillate as a function of time (where  $m \neq m'$ ).

We will now show that the dc limit of Eq. (15) contains all the information of the energy dependent transmission of the underlying relativistic quantum dynamics. In that limit, only terms with  $m = m'$  survive in Eq. (15) and the differential conductance reads

$$G = \frac{4e^2}{h} \frac{W}{\pi} \int_0^{q_{\max}} dq \sum_{m=-\infty}^{\infty} J_m^2 \left( \frac{eV_{ac}}{\hbar\omega} \right) |t_m(\varepsilon = eV)|^2. \quad (16)$$

The latter equation shows that the combination of the presence of the bias  $V$  and the ac signal  $V_{ac}$  allows to extract the energy-dependence of the transmission coefficients (in principle) channel by channel. Typical values for  $\omega$  that can be used experimentally in practice are up to 10 – 30 GHz. The bias can be controlled with any desired precision relative to  $k_B T$  down to mK temperature.

Furthermore, we find that  $G$  has an interesting feature which might give rise to potential applications. As illustrated in Fig. 2, steps appear in  $dG/dV$  if the bias  $V$  equals multiples of the ac frequency  $\omega$ . The steps show up whenever the number of propagating modes in a side band  $m$  vanishes. That is when the corresponding en-

ergy of charge carriers hits the Dirac point, where the density of states vanishes. The magnitude of the steps depends on the weight of the different side bands (given by the Bessel functions) and is non-universal. Nevertheless, the appearance of these steps can be used as a sensitive detector for finite frequency noise, similar to the SIS junction in Ref. [20]. The advantage of graphene as a finite frequency noise detector is that it has no frequency limit, whereas the SIS detector is limited by the size of the superconducting gap.

At this point, we mention that our results are obtained using scattering theory of non-interacting Dirac fermions. As shown by Pedersen and Büttiker [28] (for the corresponding problem based on the Schrödinger equation) screening of near-by gates can change the predictions of a scattering theory based on non-interacting particles. Although screening is expected to be reduced close to the Dirac point in graphene [29], where the interesting predictions illustrated in Fig. 2 appear, a careful analysis of mesoscopic ac transport in graphene in the presence of screening by near-by gates is an interesting research project by itself.

#### IV. RELATION TO ZITTERBEWEGUNG

Let us first explain the signature of ZB in the current in the absence of an oscillating potential (as introduced in Eq. (2)) and then show why our particular choice of the oscillating potential has some relevance as far as ZB is concerned. In the absence of the potential  $\mu(x)$ , the time evolution of the electron field operator that obeys Eq. (1) can be written as

$$\Psi_{\mathbf{p}}(t) = \frac{1}{2} \left[ \Psi_{\mathbf{p}}^{(+)}(t) + \Psi_{\mathbf{p}}^{(-)}(t) \right] \quad (17)$$

with  $\mathbf{p} = (p_x, p_y)$ ,  $p = \sqrt{p_x^2 + p_y^2}$ , and

$$\Psi_{\mathbf{p}}^{(\pm)}(t) = e^{\mp i v_F p t / \hbar} (1 \pm (\mathbf{p} \cdot \vec{\sigma})/p) \Psi_{\mathbf{p}},$$

where  $\vec{\sigma} = (\sigma_x, \sigma_y)$  is a vector of Pauli matrices. A straightforward calculation of the current operator in the Heisenberg picture [6] shows that an oscillatory component in time exists due to an interference of  $\Psi_{\mathbf{p}}^{(+)}(t)$  and  $\Psi_{\mathbf{p}}^{(-)}(t)$  solutions of the DE. Therefore, in order to see a signature of ZB in the current, it is important that electron-like and hole-like solutions interfere. More generally, an oscillatory component of the current arises if the electron field operator contains solutions to the DE at different energies. Consequently, if we calculated the current operator corresponding to a wave function solution to the DE with a fixed energy  $\varepsilon$ , then there would

be no oscillatory component of the current operator left and, thus, no sign of ZB in the current. Importantly, this is the general situation in ballistic transport in graphene if a plane wave solution (of a particle with energy  $\varepsilon$ ) to the DE is injected from one region to another. Thus, we conclude that ballistic dc transport in graphene shows no direct signature of ZB.

In principle, the Tien-Gordon setup of photon-assisted electron transport for Dirac electrons, illustrated in Fig. 1, can be used to generate the desired state. The reason is that the ac signal stimulates the absorption and emission of photons, which in turn lead to a population of different side bands around the Fermi energy. Then, the resulting electron field operator in region  $Gr(in)$ , Eq. (10), is precisely what is needed to observe ZB in graphene. However, the detection of the resulting oscillating current, Eq. (15), is not sufficient to prove the existence of ZB in graphene. The reason is that a preparation of a state that is a superposition of different energy solutions to the free Schrödinger equation also yields a similar oscillating current (see, for instance, Eq. (16) of Ref. [28]). The only difference to the free Schrödinger case as compared to the Dirac case is the peculiar energy dependence of the transmission in the latter. Therefore, the Tien-Gordon setup analyzed in this paper is potentially relevant to the detection of ZB, but our analysis indicates that the truly fundamental signature of ZB needs to be identified more precisely.

#### V. CONCLUSIONS

We have emphasized in this article that the energy dependence of the transmission (typical for mesoscopic graphene systems) plays a crucial role for the unexpected transport phenomena predicted in these devices, for recent examples see Refs. [6, 9, 10, 11, 12, 13, 14, 15]. Therefore, it is desirable to directly probe the energy dependence of the transmission. We have demonstrated that photon-assisted transport is the natural way to do so. Furthermore, we have pointed out that a possible application of our setup is to use graphene as a spectrometer for finite frequency noise. Finally, we have discussed the relevance of photon-assisted transport in graphene to the observability of ZB. Our conclusion is that photon-assisted transport can be used to create the conditions to observe ZB. However, our analysis also shows that the truly fundamental signature of ZB (which is important for its detection) needs to be pinpointed in future studies.

We thank C.W.J. Beenakker, H. Heersche, P. Jarillo-Herrero, J. Schliemann, I. Snyman, and L.M.K. Vander-sypen for interesting discussions. This research was supported by the Dutch Science Foundation NWO/FOM.

---

[1] K. S. Novoselov, A. K. Geim, S.V. Morozov, D. Jiang, M. I. Katsnelson, I. V. Grigorieva, S. V. Dubonos, and

A. A. Firsov, Nature **438**, 197 (2005).

- [2] Y. Zhang, Y.-W. Tan, H. L. Stormer, and P. Kim, *Nature* **438**, 201 (2005).
- [3] A. W. W. Ludwig, M. P. A. Fisher, R. Shankar, and G. Grinstein, *Phys. Rev. B* **50**, 7526 (1994).
- [4] K. Ziegler, *Phys. Rev. Lett.* **80**, 3113 (1998).
- [5] N. M. R. Peres, F. Guinea, and A. H. Castro Neto, *Phys. Rev. B* **73**, 125411 (2006).
- [6] M. I. Katsnelson, *Eur. Phys. J. B* **51**, 157 (2006).
- [7] K. Nomura and A.H. MacDonald, *cond-mat/0606589*.
- [8] P. M. Ostrovsky, I. V. Gornyi, and A. D. Mirlin, *cond-mat/0609617*.
- [9] J. Tworzydło, B. Trauzettel, M. Titov, A. Rycerz, and C. W. J. Beenakker, *Phys. Rev. Lett.* **96**, 246802 (2006).
- [10] V. V. Cheianov and V. I. Falko, *Phys. Rev. B* **74**, 041403(R) (2006).
- [11] M. I. Katsnelson, K. S. Novoselov, and A. K. Geim, *Nature Phys.* **2**, 620 (2006).
- [12] C. W. J. Beenakker, *Phys. Rev. Lett.* **97**, 067007 (2006).
- [13] M. Titov and C. W. J. Beenakker, *Phys. Rev. B* **74**, 041401(R) (2006).
- [14] J. C. Cuevas and A. Levy Yeyati, *cond-mat/0609138*.
- [15] M. Titov, A. Ossipov, and C. W. J. Beenakker, *cond-mat/0609623*.
- [16] V. P. Gusynin, S. G. Sharapov, and J. P. Carbotte, *Phys. Rev. Lett.* **96**, 256802 (2006).
- [17] P. K. Tien and J. P. Gordon, *Phys. Rev.* **129**, 647 (1963).
- [18] For a recent review, see G. Platero and R. Aguado, *Phys. Rep.* **395**, 1 (2004).
- [19] A similar effect to the one we discuss in this article is seen if the ac signal is applied to the bias rather than to the gate. Both ways are feasible from an experimental point of view.
- [20] R. Deblock, E. Onac, L. Gurevich, and L. P. Kouwenhoven, *Science* **301**, 203 (2003).
- [21] E. Schrödinger, *Sitzungsber. Preuss. Akad. Wiss., Phys. Math. Kl.* **24**, 418 (1930).
- [22] K. Huang, *Am. J. Phys.* **20**, 479 (1952).
- [23] J. Schliemann, D. Loss, and R. M. Westervelt, *Phys. Rev. Lett.* **94**, 206801 (2005); *Phys. Rev. B* **73**, 085323 (2006).
- [24] W. Zawadzki, *cond-mat/0510184*.
- [25] J. Cserti and G. David, *cond-mat/0604526*.
- [26] T. M. Rusin and W. Zawadzki, *cond-mat/0605384*.
- [27] R. Winkler, U. Zülicke, and J. Bolte, *cond-mat/0609005*.
- [28] M. H. Pedersen and M. Büttiker, *Phys. Rev. B* **58**, 12993 (1998).
- [29] D. P. DiVincenzo and E. J. Mele, *Phys. Rev. B* **29**, 1685 (1984).